Electron-capture delayed fission properties of ^{244}Es

D. A. Shaughnessy, K. E. Gregorich , J. L. Adams, M. R. Lane*, C. A. Laue†, D. M. Lee, C. A. McGrath‡, V. Ninov, J. B. Patin, D. A. Strellis§, E. R. Sylwester‖, P. A. Wilk, and D. C. Hoffman

Nuclear Science Division, Lawrence Berkeley National Laboratory, MS 70A-1150, Berkeley, California 94720 and Chemistry Department, University of California, Berkeley, California 94720

PACS number(s): 21.10.Gv, 23.40.-s, 25.70.Gh, 27.90.+b

Electron-capture delayed fission was observed in ^{244}Es produced via the ^{237}Np(^{12}C,5n)^{244}Es reaction at 81 MeV (on target) with a production cross section of 0.31±0.12 μb. The mass-yield distribution of the fission fragments is highly asymmetric. The average pre-neutron-emission total kinetic energy of the fragments was measured to be 186±19 MeV. Based on the ratio of the number of fission events to the measured number of α decays from the electron-capture daughter ^{244}Cf (100% α branch), the probability of delayed fission was determined to be $(1.2\pm0.4) \times 10^{-4}$. This value for the delayed fission probability fits the experimentally observed trend of increasing delayed fission probability with increasing Q value for electron-capture.

---

* Present address: The College Preparatory School, Oakland, CA 94618.
† Present address: Lawrence Livermore National Laboratory, L-231, Livermore, CA 94551.
‡ Present address: Idaho National Engineering and Environmental Laboratory, Idaho Falls, ID 83415.
§ Present address: Ancore Corp., 2950 Patrick Henry Dr., Santa Clara, CA 95054.
‖ Present address: Glenn T. Seaborg Institute for Transactinium Science, L-231, Lawrence Livermore National Laboratory, Livermore, CA 94551.

I. INTRODUCTION

Electron-capture delayed fission (ECDF) is a nuclear decay mode whereby a parent nucleus undergoes electron-capture (EC) decay, populating excited states in the daughter nucleus, which then fission. The ECDF process is illustrated in Fig. 1. The excited states in the daughter nucleus that are populated through the initial EC decay can be above the fission barrier, resulting in prompt fission, within the second well of the potential energy surface, yielding a fission shape isomer, or inside the first well of the potential energy surface, where the nucleus is more likely to deexcite via γ transitions. The ECDF decay mode is of special interest because it allows study of the fission properties of the daughter nucleus, which would normally have a ground state spontaneous fission branch too small for detailed investigation. Delayed fission (DF) is also thought to play an important role in determining the yields of heavy elements produced in multiple neutron capture processes such as the astrophysical r-process and in nuclear weapons tests [1-5]. For a more complete description of the DF process, see Refs. [6-9] and the references therein.

The probability of undergoing ECDF (P_{DF}) is defined as the ratio of the number of EC decays resulting in fission, N_{ECDF}, to the total number of EC events, N_{EC}:

$$P_{DF} = \frac{N_{ECDF}}{N_{EC}}.$$

ECDF has been previously reported in the neutron deficient neptunium [10,11], americium [7,8,12,13], berkelium [10,13,14], and einsteinium [10,13,15-17] regions. This decay mode is expected to have measurable branches in nuclides where the electron-capture Q-value (Q_{EC}) is comparable to the height of the fission barrier in the daughter nucleus. Nuclides that meet this requirement are found in neutron-deficient actinides that have odd numbers of protons and neutrons. These odd-odd nuclei have enhanced Q_{EC} values associated with EC decay to their more stable even-even daughter nuclei. The Q_{EC} for ^{244}Es is 4.36 MeV [18], which approaches the estimated fission barrier heights of 5-7 MeV for this region [19]. Previous experiments have shown that the P_{DF} increases with increasing Q_{EC} [9,11,14,16, 17].

^{244}Es was first identified by Eskola [20] during an experiment in which ^{233}U was bombarded with ^{15}N projectiles. This paper was a preliminary report, but ^{244}Es was said to decay with a 100% EC branch and a half-life of 40±5 s. This dominant EC branch was confirmed when no ^{244}Es α particles were observed during an experiment in which ^{241}Am was bombarded with ^{12}C projectiles to look for isotopes of mendelevium and their einsteinium daughters [21]. A final paper by Eskola *et al*. reported α particles from the decay of ^{244}Es produced via the ^{233}U(^{15}N,4n)^{244}Es reaction at projectile energies of 77-82 MeV [22]. They assigned an α energy of 7.57±0.02 MeV, an α branch of 4^{+3}_{-2}%, and a half-life of 37±4 s to ^{244}Es.

ECDF in ^{244}Es was first reported by Gangrskii *et al*. [13]. The nuclide was produced both via the ^{233}U(^{14}N,5n)^{244}Es and ^{237}Np(^{12}C,5n)^{244}Es reactions at projectile energies of 82-86 MeV. The production cross section was reported to be 1 μb but it was not specified with which reaction this cross section was associated. A P_{DF} of 10^{-4} was determined by comparing the number of fission events observed in a solid-state fission track detector to the number of α-decay events from the ^{244}Cf EC daughter. The total number of ^{244}Es EC events was determined from the number of daughter events by assuming a 100% EC branch in ^{244}Es. No errors were given for this reported P_{DF} value. Also, the fission properties of the ^{244}Cf daughter were not determined. Therefore, we decided to measure the ECDF of ^{244}Es in order to better evaluate its P_{DF} value and to determine the fission properties of its EC daughter.

II. EXPERIMENTAL TECHNIQUES

A. Targets and irradiation

An aqueous solution containing 1.61 mg of ^{237}Np was sorbed onto a 7.5-mm by 27.5-mm anion exchange column (AG 1X-8 resin, 200-400 mesh) and rinsed with concentrated HCl to remove lead and other impurities. A small amount of ^{239}Pu that was present in the original solution was removed from the column by eluting with a 7:1 solution of concentrated HCl:HI. Any residual HI was removed by rinsing the column with concentrated HCl, and the ^{237}Np was eluted with 2 M HCl. The resulting solution, which contained 480 μg of ^{237}Np, was evaporated to dryness and dissolved in 1 mL of isopropyl alcohol (IPA) to yield a solution that was approximately 0.5 mg/mL in ^{237}Np. Successive target layers were produced by electroplating aliquots containing 25 μg of ^{237}Np from 1.25 mL of IPA in a 6-mm diameter circle onto a 0.5-mil (2.32 mg/cm^2) Be foil at 300 V (0.7 mA) for 30 min. The ^{237}Np was then converted to the oxide by baking each layer in a 450°C oven for 30 min. The thickness of the target was determined via α analysis using a surface barrier detector operated under vacuum with a detection efficiency of 34%, and was found to be 487.5 μg/cm^2. The target configuration has been described elsewhere [23].

A 3.0-μA ^{12}C^{4+} beam (81 MeV in the lab system at the entrance to the target) was provided by the 88-Inch Cyclotron at Lawrence Berkeley National Laboratory. During bombardment, reaction products were swept from the target chamber, attached to KCl aerosols from a He/KCl gas-jet, and then transported via a 1.4-mm i.d. Teflon capillary to our rotating wheel detection system [24] for α and fission measurements.

B. Measurements of α and fission activity

On-line measurements of α particles and fission fragments were made in our Merry-Go-Around (MG) rotating wheel detection system [24]. This rotating horizontal wheel, on-line, continuous collection and detection system, has been previously described by Hoffman *et al.*

[24]. The activity-laden KCl aerosols were deposited via the He/KCl gas-jet successively onto 80 thin polypropylene foils (40±10 μg/cm^2) supported on 0.63-mm i.d. rings positioned around the periphery of a 51-cm diameter fiberglass wheel. There were 80 collection sites on each wheel, but only 79 were used during a given experiment. The transport efficiency of the gas-jet system was estimated to be 60±20% based on previous experiments [25]. Six pairs of passivated ion implanted silicon (PIPS) detectors were situated directly above and below the wheel to measure the kinetic energy of α particles and coincident fission fragments. The horizontal wheel was rotated every 30 s so as to move the first foil from the collection site into position for counting between the first detector pair while collection proceeded concurrently on a new foil. Each step of the wheel moved a new foil into the collection position and the collected samples were moved successively between the six pairs of detectors so that each collection was counted for a total time equivalent to 180 s. With this system, collection and counting are essentially continuous since the time required to move the wheel (~ 0.1 s) is much less than the stepping interval. The detection efficiency in any given detector was approximately 32% for α particles and 64% for fission fragments.

After 80 min of continuous collection and measurement (two complete revolutions of the wheel), the last six collections were stopped under the detector pairs and counted while the wheel was stationary for an additional 40 min. During this time interval, the longer-lived daughter activity was measured after the shorter-lived interfering activities had decayed away. After that time, the wheel was replaced with a clean one to prevent the buildup of KCl on the foils, which would worsen the α resolution during the experiment, and also prevented the buildup of any longer-lived fission activities. This entire process was continually repeated over the course of 36 h of beam time.

Data were collected using the GOOSY data acquisition system [26]. Calibrations were performed before the experiment using a ^{212}Pb source, which provided 6.062-MeV and 8.784-MeV α particles, and a ^{252}Cf source was used for fission fragment energies. The energy resolution [full width at half maximum (FWHM)] of the detectors positioned above the wheel was approximately 0.04 MeV and the detectors below the wheel had a resolution of approximately 0.1 MeV due to energy degradation of the α particles as they traveled through the polypropylene foil en route to the bottom detectors. The fission background was measured prior to the start and at the termination of the experiment and was less than one fission event per detector per day.

III. RESULTS AND DISCUSSION

A. Fission properties and half-life

A total of 13 pairs of coincident fission fragments were detected over the course of the entire experiment. Subsequent analysis of the data showed that at some point during the experiment the first detector pair had stopped working. Only two coincident fission events were detected in the first pair instead of the approximately 10 we would expect based on the subsequent decay curve of fission events. The two events from detector pair one were removed from the half-life analysis but were included in determining fission properties. Two components were evident in the fission decay curve, the shorter ^{244}Es component, with an initial activity (A_o) of 0.216 fissions/s, and a longer-lived activity, which was fixed at 0.05 fissions/s. A nonlinear least-squares two-component fit to the coincident fission events resulted in a half-life of 31±10 s for the shorter component, which indicates that the events came from the delayed fission of ^{244}Es. The fission process is very fast compared to the initial EC decay and the fission events therefore decay with the half-life of the EC parent. This half-life is consistent with the reported value of 37±4 s for ^{244}Es [22].

Fission fragment energy calibrations were based on the spontaneous fission of ^{252}Cf, and were obtained using the method of Schmitt, Kiker, and Williams [27] using the constants of Weissenberger *et al*. [28]. 78.4 MeV and 102.6 MeV were used for the most probable low and high peak energies in the spontaneous fission of ^{252}Cf, respectively. The average neutron emission function, $\bar{\nu}(A)$, was assumed to be similar to that of ^{252}Cf, normalized to an average neutron emission $\overline{\nu_t} = 2.6$, estimated from systematics in Ref. [29]. Since fission events in ECDF are preceded by EC decays, the fission properties measured during the experiment are for the EC daughter, ^{244}Cf. Figure 2 shows the highly asymmetric mass-yield distribution of fission fragments for ^{244}Cf. The mass-yield data are expressed as yield (%) per mass number with the fragment yield normalized to 200%, and are derived from the ratio of the kinetic energies of both fragments for each coincident fission fragment pair.

The average pre-neutron-emission total kinetic energy (TKE) for coincident fission fragments from ^{244}Cf was measured to be 186±19 MeV. The most probable light fragment energy was determined to be 78.6±10.4 MeV and the most probable heavy fragment energy was 107±10 MeV. From these fragment energies, it was determined that the mass (A) of the light fragment was 103 while the heavy fragment had a mass of A=141. Since the ^{252}Cf calibration source was measured on the same kind of polypropylene foil used on the MG wheels during the experiment, no correction was made for energy degradation of fission fragments as they traveled through the foils to the bottom detectors. Also, no correction was made for the approximately 15 μg/cm^2 of KCl aerosol [30] deposited on each foil by the gas-jet transport system because typical fission fragments only lose 0.2-0.4 MeV of energy [31] as they travel through this amount of

KCl to the detectors. Figure 3 shows the average or most probable TKE versus $Z^2/A^{1/3}$ for all known spontaneous fission and delayed fission isotopes, as well as the empirical fits of Viola *et al*. [32] and Unik *et al*. [33]. The average TKE value of 186±19 MeV agrees within error with these empirical predictions and appears to follow the trend of TKE values measured in other ECDF systems.

According to the static fission model of Wilkins *et al*. [34] actinides with neutron number greater than 140 should have asymmetric mass splits until the Fm region is reached. The heavy fragment in the split should remain nearly constant around either the $N=82$ (spherical) or $N\approx88$ (deformed) neutron shell. If the heavy fragment is located around the spherical neutron shell, then the complementary fragment is forced to be highly deformed. In order to maintain the N/Z ratio of the fissioning nucleus, the heavy fragment in the fission of ^{244}Cf ($A = 141$) would be nearly spherical with $N = 82$ ($Z = 56$, $\beta = 0.2$ where β is the nuclear deformation parameter from Ref. [34]), and its complement would therefore be highly deformed with $N = 64$ ($Z = 42$, $\beta \approx 0.9$ [34].) A symmetric split would result in two fragments with $Z = 49$ and $N = 73$. The presence of the $Z = 50$ spherical proton shell might suggest a symmetric component in the fission of ^{244}Cf, but there are no corresponding neutron shells around $N = 73$, which means both fragments would have deformations greater than $\beta = 0.25$. This in turn removes the protons from the spherical shell, causing the fragments to become more deformed. A symmetric split would therefore consist of two deformed fragments, resulting in a lower TKE than in the case of one nearly spherical fragment and one highly deformed fragment. As shown in Fig. 2, the mass-yield distribution shows no evidence of a symmetric component, indicating that the fission of ^{244}Cf prefers an asymmetric fragment configuration consisting of one nearly spherical fragment and one highly deformed fragment rather than two deformed fragments.

B. P_{DF}

Figure 4(a) shows the summed α-spectrum taken from all of the MG wheels measured during the experiment in the top detector of the first detector pair (36 h of beam time.) The interfering activities in the spectrum arise from the interaction of the ^{12}C beam with lead impurities in the ^{237}Np target. A peak was observed at 7.580 MeV and was believed to be ^{244}Es based on the α energy reported by Eskola *et al.* [22]. However, a half-life analysis of the peak area over time using a nonlinear least-squares fit did not identify a 37-s activity that could be assigned to ^{244}Es. The tail of the larger, neighboring ^{245}Es peak probably obscures any α particles from the decay of ^{244}Es. In order to determine the P_{DF} of ^{244}Es, we instead looked at the spectra recorded when the wheel was stationary to identify ^{244}Cf, the EC daughter of ^{244}Es.

Figure 4(b) represents the summed spectrum of all measurements made in the top detector of the sixth detector pair while the wheel was stationary (approximately 13 h of counting.) The sample in detector pair six had the longest delay between collection and the start of counting (150 s), which allowed most of the shorter-lived interfering activities to decay before counting began. ^{244}Cf has a half-life of 19.4 min and α energies of 7.213 and 7.176 MeV with a 100% α decay branch [31]. By incorporating both α-particle energies in our analysis of the ^{244}Cf peak, the number of ^{244}Cf α particles detected was equal to the total number of ^{244}Es EC decays, after applying a small correction for the 4% α branch in ^{244}Es [22]. We neglected the direct production of ^{244}Cf via the ^{237}Np(^{12}C,p4n)^{244}Cf reaction because of its low cross section. Based on information in Refs. [13] and [35] we assumed that the production of ^{244}Cf via the p4n exit channel was less than 10% of the 5n exit channel, which is well within the standard deviation of our subsequent P_{DF} measurement. Based on the total number of ^{244}Es EC decays, a production cross section of 0.31±0.12 μb was calculated for the ^{237}Np(^{12}C,5n)^{244}Es reaction at a beam energy of 81 MeV in the lab system (on target.) Experimental uncertainties, including the yield of the He gas-jet transport system, fluctuations in beam intensity, nonuniformity of target thickness, and detection efficiency, have all been taken into account in the determination of this cross section and its standard deviation.

From the 20 single fission events (non-coincident) and 382 ^{244}Cf α particles detected over the course of the experiment (these values were later normalized to the number of samples collected), a P_{DF} of (1.2±0.4) x 10^{-4} was determined using the equation given in Sec. I. Because the α particles and fission fragments were measured from the same samples, experimental uncertainties in N_{ECDF} and N_{EC} canceled out in the calculation of the P_{DF}. Variations in beam intensity, target thickness, detection efficiency, and yield of the He gas-jet transport system were small from one collection to another and were much less than the standard deviation of our measurement. Therefore, only statistical uncertainties in the numbers of α particles and fission events were considered in the P_{DF}. Our value for the P_{DF} of ^{244}Es of (1.2±0.4) x 10^{-4} with a Q_{EC} of 4.36 MeV [18] for ^{244}Es fits the empirical relationship between P_{DF} and Q_{EC} shown in Fig. 5.

IV. CONCLUSIONS

ECDF was observed in ^{244}Es produced via the ^{237}Np(^{12}C,5n)^{244}Es reaction using an 81-MeV ^{12}C beam (on target.) The fission properties were measured using our rotating wheel detection system. The mass-yield distribution of fragments from the fission of ^{244}Cf was highly asymmetric as expected for low-energy fission in this region. Based on the deformation diagrams of Wilkins *et al.* [34], the heavy fragment in the fission of ^{244}Cf is most likely nearly spherical, forcing the complementary fragment to be highly deformed.

The average pre-neutron-emission TKE of the fission fragments was 186±19 MeV. As seen in Fig. 3, the TKE values measured for ECDF systems all appear to be lower than those reported for spontaneous fission isotopes. However, more precise measurements are needed to determine whether this is an actual phenomenon related to the delayed fission process.

A P_{DF} of $(1.2\pm0.4) \times 10^{-4}$ was calculated from the delayed fission events and the α decay of the EC daughter ^{244}Cf. The line in Fig. 5 represents a nonlinear least-squares fit to the P_{DF} values that have been previously determined by our research group. It appears that the P_{DF} is directly dependent on the Q_{EC}. As the Q value increases, the daughter nucleus is left in an excited state that is closer to the height of the fission barrier. Fission barriers in this region do not vary greatly with neutron number [19]; therefore, the P_{DF} must have a strong dependence on the Q_{EC} since fission barrier heights are not changing enough to account for such a broad range of P_{DF} values. A larger Q_{EC} means that the daughter nucleus has a better chance to overcome its fission barrier, thereby increasing the probability that it will undergo fission. Since the P_{DF} is a measure of probability, it can never be greater than one. Future experiments should be made to try to determine the shape of the P_{DF} function in Fig. 5 at higher Q values. By examining systems with larger Q values, it can be determined whether this function keeps increasing toward a value of one, or whether it levels off at some maximum P_{DF} value.

ACKNOWLEDGMENTS

The authors wish to thank the staff and operators of the 88-Inch Cyclotron at Lawrence Berkeley National Laboratory for providing the ^{12}C beams. This work was supported in part by the Director, Office of Science, Office of High Energy and Nuclear Physics, Division of Nuclear Physics, U.S. Department of Energy under Contract No. DE-AC03-76SF00098.

[1] E. M. Burbidge, G. R. Burbidge, W. A. Fowler and F. Hoyle, Rev. Mod. Phys. **29**, 547 (1957).

[2] C.-O. Wene, Astron. Astrophys. **44**, 233 (1975).

[3] C.-O. Wene and S. A. E. Johansson, Phys. Scr. **A10**, 156 (1974).

[4] H. V. Klapdor, T. Oda, J. Metzinger, W. Hillebrand, and F. K. Thielemann, Z. Phys. A 299, 213 (1981).

[5] B. S. Meyer, W. M. Howard, G. J. Matthews, K. Takahashi, P. Möller, and G. Leander, Phys. Rev. C **39**, 1876 (1989).

[6] E. E. Berlovich and Yu. P. Novikov, Sov. Phys. Dokl. **14**, 349 (1969).

[7] H. L. Hall, K. E. Gregorich, R. A. Henderson, C. M. Gannett, R. B. Chadwick, J. D. Leyba, K. R. Czerwinski, B. Kadkhodayan, S. A. Kreek, D. M. Lee, M. J. Nurmia, D. C. Hoffman, C. E. A. Palmer, and P. A. Baisden, Phys. Rev. C **41**, 618 (1990).

[8] H. L. Hall, K. E. Gregorich, R. A. Henderson, C. M. Gannett, R. B. Chadwick, J. D. Leyba, K. R. Czerwinski, B. Kadkhodayan, S. A. Kreek, N. J. Hannink, D. M. Lee, M. J. Nurmia, D. C. Hoffman, C. E. A. Palmer, and P. A. Baisden, Phys. Rev. C **42**, 1480 (1990).

[9] H. L. Hall and D. C. Hoffman, Annu. Rev. Nucl. Part. Sci. **42**, 147 (1992).

[10] D. Habs, H. Klewe-Nebenius, V. Metag, B. Neumann, and H. J. Specht, Z. Phys. A **285**, 53 (1978).

[11] S. A. Kreek, H. L. Hall, K. E. Gregorich, R. A. Henderson, J. D. Leyba, K. R. Czerwinski, B. Kadkhodayan, M. P. Neu, C. D. Kacher, T. M. Hamilton, M. R. Lane, E. R. Sylwester, A. Türler, D. M. Lee, M. J. Nurmia, and D. C. Hoffman, Phys. Rev. C **50**, 2288 (1994).

[12] H. L. Hall, K. E. Gregorich, R. A. Henderson, C. M. Gannett, R. B. Chadwick, J. D. Leyba, K. R. Czerwinski, B. Kadkhodayan, S. A. Kreek, D. M. Lee, M. J. Nurmia, and D. C. Hoffman, Phys. Rev. Lett. **63**, 2548 (1989).

[13] Yu. P. Gangrskii, M. B. Miller, L. V. Mikhailov, and I. F. Kharisov, Sov. J. Nucl. Phys. **31**, 162 (1980).

[14] S. A. Kreek, H. L. Hall, K. E. Gregorich, R. A. Henderson, J. D. Leyba, K. R. Czerwinski, B. Kadkhodayan, M. P. Neu, C. D. Kacher, T. M. Hamilton, M. R. Lane, E. R. Sylwester, A. Türler, D. M. Lee, M. J. Nurmia, and D. C. Hoffman, Phys. Rev. C **49**, 1859 (1994).

[15] R. Hingmann, W. Kühn, V. Metag, R. Novotny, A. Ruckelshausen, H. Ströher, F. Hessberger, S. Hofmann, G. Münzenberg, and W. Reisdorf, Gesellschaft für Schwerionenforschung, Darmstadt, Report No. GSI 85-1, 88 (1985).

[16] D. A. Shaughnessy, J. L. Adams, K. E. Gregorich, M. R. Lane, C. A. Laue, D. M. Lee, C. A. McGrath, J. B. Patin, D. A. Strellis, E. R. Sylwester, P. A. Wilk, and D. C. Hoffman, Phys. Rev. C **61**, 044609 (2000).

[17] D. A. Shaughnessy, K. E. Gregorich, M. R. Lane, C. A. Laue, D. M. Lee, C. A. McGrath, D. A. Strellis, E. R. Sylwester, P. A. Wilk, and D. C. Hoffman, Phys. Rev. C **63**, 037603 (2001).

[18] P. Möller, J. R. Nix, W. D. Myers, and W. J. Swiatecki, Atomic Data Nucl. Data Tables **59**, 185 (1995).

[19] H. C. Britt, E. Cheifetz, D. C. Hoffman, J. B. Wilhelmy, R. J. Dupzyk, and R. W. Lougheed, Phys. Rev. C **21**, 761 (1980).

[20] P. Eskola, Lawrence Radiation Laboratory Nuclear Chemistry Annual Report UCRL-2-426 (1970).

[21] P. Eskola, Phys. Rev. C **7**, 280 (1973).

[22] P. Eskola, K. Eskola, M. Nurmia, and A. Ghiorso, Phys. Fenn. **8**, 357 (1973).

[23] M. R. Lane, K. E. Gregorich, D. M. Lee, B. Wierczinski, C. A. McGrath, M. B. Hendricks, D. A. Shaughnessy, D. A. Strellis, E. R. Sylwester, P. A. Wilk, and D. C. Hoffman, Phys. Rev. C **58**, 3413 (1998).

[24] D. C. Hoffman, D. M. Lee, K. E. Gregoich, M. J. Nurmia, R. B. Chadwick, K. B. Chen, K. R. Czerwinski, C. M. Gannett, H. L. Hall, R. A. Henderson, B. Kadkhodayan, S. A. Kreek, and J. D. Leyba, Phys. Rev. C **41**, 631 (1990).

[25] P. A. Wilk, K. E. Gregorich, M. B. Hendricks, M. R. Lane, D. M. Lee, C. A. McGrath, D. A. Shaughnessy, D. A. Strellis, E. R. Sylwester, and D. C. Hoffman, Phys. Rev. C **56**, 1626 (1997).

[26] V. Ninov, private communication (1998).

[27] H. W. Schmitt, W. E. Kiker, and C. W. Williams, Phys. Rev. **137**, B837 (1965).

[28] E. Weissenberger, P. Geltenbort, A. Oed, F. Gönnenwein, and H. Faust, Nucl. Instrum. Methods Phys. Res. A **248**, 506 (1986).

[29] D. C. Hoffman and M. M. Hoffman, Annu. Rev. Nucl. Sci. **24**, 151 (1974).

[30] S. A. Kreek, H. L. Hall, K. E. Gregorich, R. A. Henderson, J. D. Leyba, K. R. Czerwinski, B. Kadkhodayan, M. P. Neu, C. D. Kacher, T. M. Hamilton, M. R. Lane, E. R. Sylwester, A. Türler, D. M. Lee, M. J. Nurmia, and D. C. Hoffman, Phys. Rev. C **50**, 2288 (1994).

[31] R. B. Firestone and V. S. Shirley, Editors, *Table of Isotopes*, 8th ed. (Wiley Interscience, New York, 1996).

[32] V. E. Viola, K. Kwiatkowski, and M. Walker, Phys. Rev. C **31**, 1550 (1985).

[33] J. P. Unik, J. E. gindler, L. E. Glendenin, K. F. Flynn, A. Gorski, and R. K. Sjoblom, in *Proceedings of the third International IAEA Symposium on the Physics and Chemistry of Fission, Rochester, 1973* (IAEA, Vienna, 1974), Vol. II, p. 19.

[34] B. D. Wilkins, E. P. Steinberg, and R. R. Chasman, Phys. Rev. C **14**, 1832 (1976).

[35] R. A. Henderson, Ph.D. thesis, University of California, Berkeley, 1990; Lawrence Berkeley Laboratory Report LBL-29568, 1990.

Figure Captions:

FIG. 1. Two-dimensional drawing of the delayed fission process. The potential energy surface of the daughter nucleus is shown, illustrating the double-humped fission barrier commonly observed in the actinides. As seen in the figure, delayed fission can occur from either a high-lying state in the first potential well, or from an isomeric state in the second well.

FIG. 2. Pre-neutron-emission mass-yield distribution for the ECDF of ^{244}Es. The fissioning species is ^{244}Cf. The data were averaged over 5 mass units.

FIG. 3. The average or most probable TKE vs $Z^2/A^{1/3}$ for known cases of spontaneous or delayed fission. The solid line is the linear fit of Viola *et al*. [32] and the dashed line is from Unik *et al*. [33]. All of the TKE values have been corrected to be consistent with the calibration parameters of Weissenberger *et al*. [28].

FIG. 4. Summed α spectra for the ^{237}Np + ^{12}C reaction at a beam energy of 81 MeV. (a) Spectrum from the first top detector recorded while the wheel was stepping for a total of 36 h. (b) Spectrum from the sixth top detector recorded while the wheel was stationary representing approximately 13 h.

FIG. 5. Plot of the ECDF probability vs. electron-capture Q-value for nuclides studied by our research group. The values for ^{232}Am and ^{234}Am are from Refs. [7,8], ^{228}Np is from Ref. [11], ^{238}Bk is from Ref. [19], ^{242}Es is from Ref. [16], and ^{246}Es and ^{248}Es are from Ref. [17].

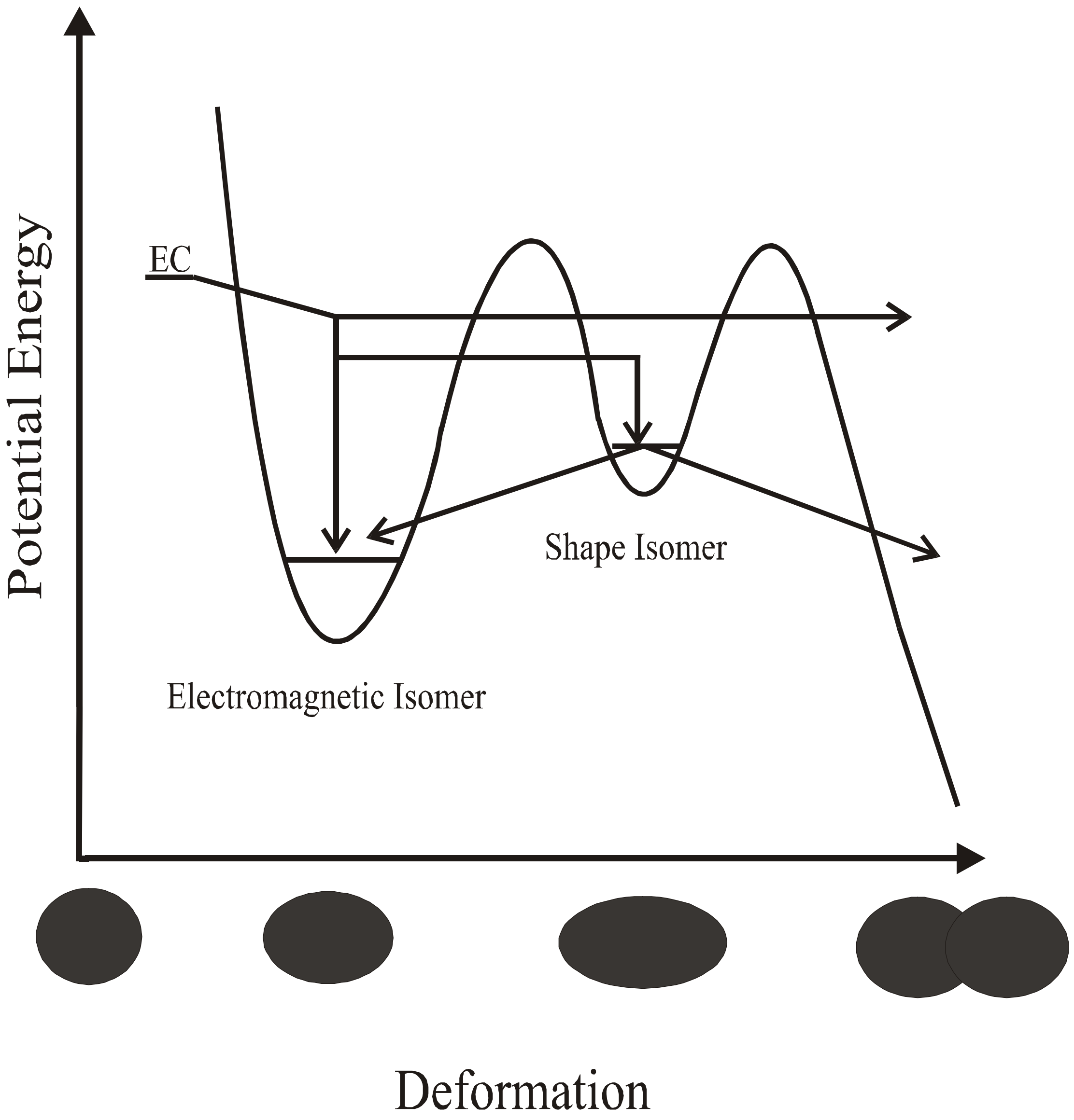
Potential Energy
EC
Shape Isomer
Electromagnetic Isomer
Deformation

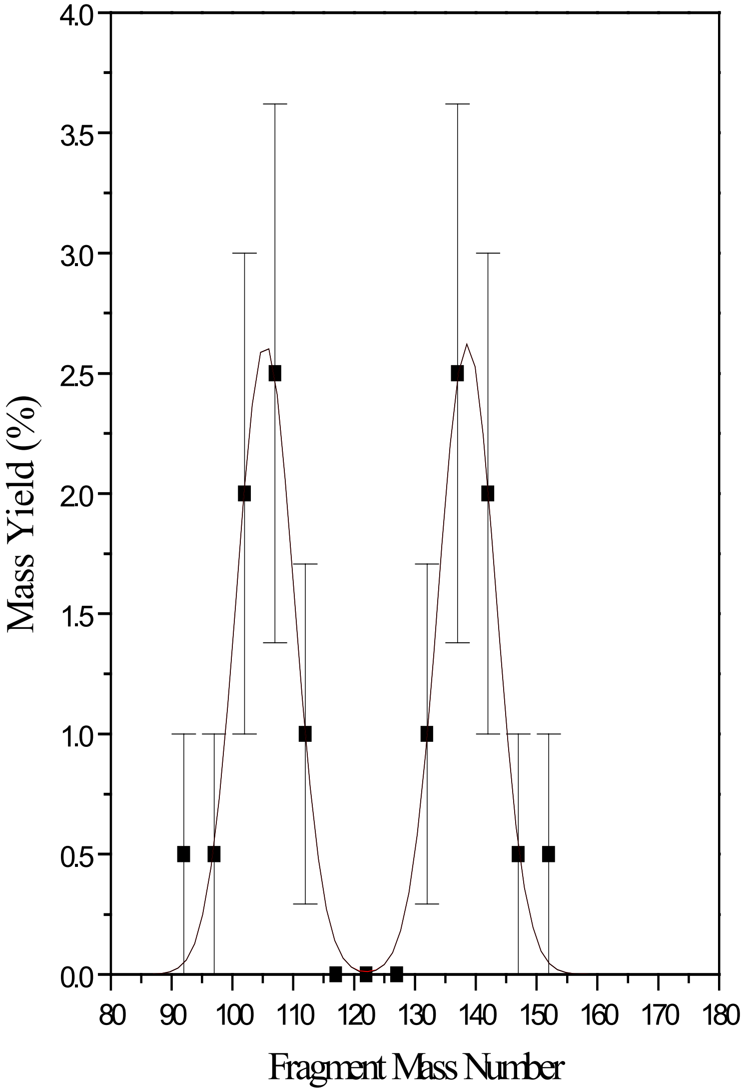

Mass Yield (%)
4.0
3.5
3.0
2.5
2.0
1.5
1.0
0.5
0.0
80
90
100
110
120
130
140
150
160
170
180
Fragment Mass Number

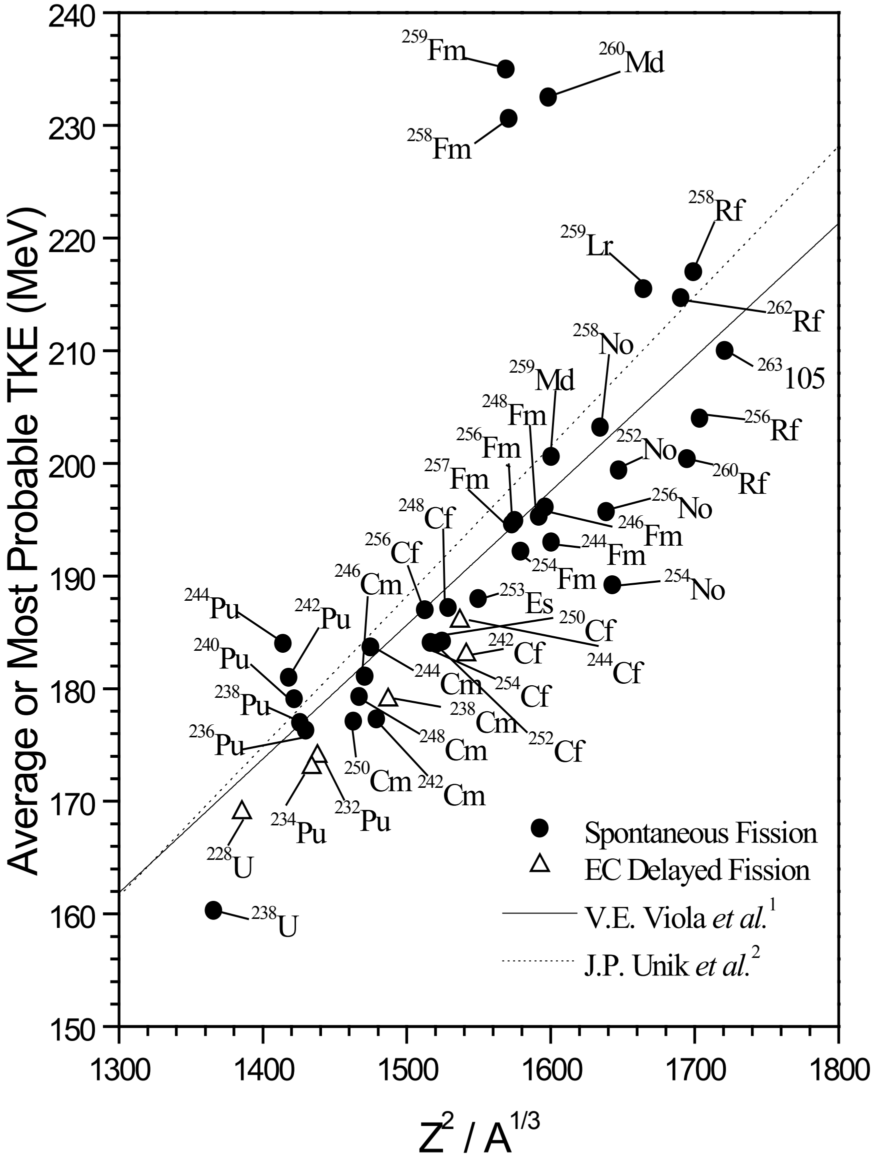

Average or Most Probable TKE (MeV)
150
160
170
180
190
200
210
220
230
240
1300
1400
1500
1600
1700
1800
$Z^2 / A^{1/3}$
^{259}Fm
^{260}Md
^{258}Fm
^{258}Rf
^{259}Lr
^{262}Rf
^{258}No
^{263}105
^{259}Md
^{248}Fm
^{256}Rf
^{256}Fm
^{252}No
^{260}Rf
^{257}Fm
^{256}No
^{248}Cf
^{246}Fm
^{244}Fm
^{256}Cf
^{254}Fm
^{254}No
^{246}Cm
^{253}Es
^{244}Pu
^{242}Pu
^{250}Cf
^{242}Cf
^{244}Cf
^{240}Pu
^{244}Cm
^{254}Cf
^{238}Pu
^{238}Cm
^{252}Cf
^{236}Pu
^{248}Cm
^{250}Cm
^{242}Cm
^{232}Pu
^{234}Pu
^{228}U
^{238}U
● Spontaneous Fission
△ EC Delayed Fission
V.E. Viola et al.[1]
J.P. Unik et al.[2]

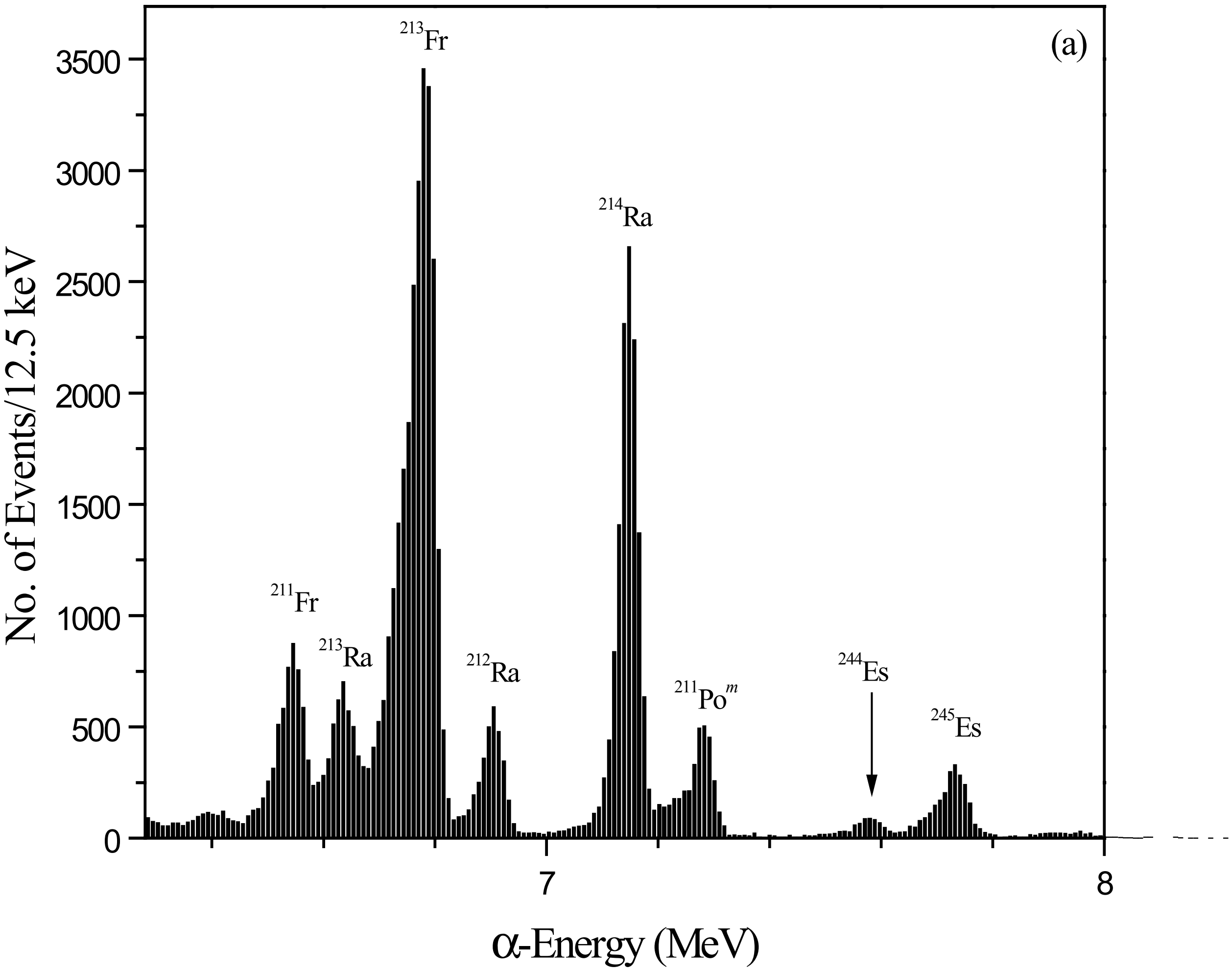
(a)
^{213}Fr
^{214}Ra
^{211}Fr
^{213}Ra
^{212}Ra
^{211}Po^m
^{244}Es
^{245}Es
No. of Events/12.5 keV
0
500
1000
1500
2000
2500
3000
3500
7
8
α-Energy (MeV)

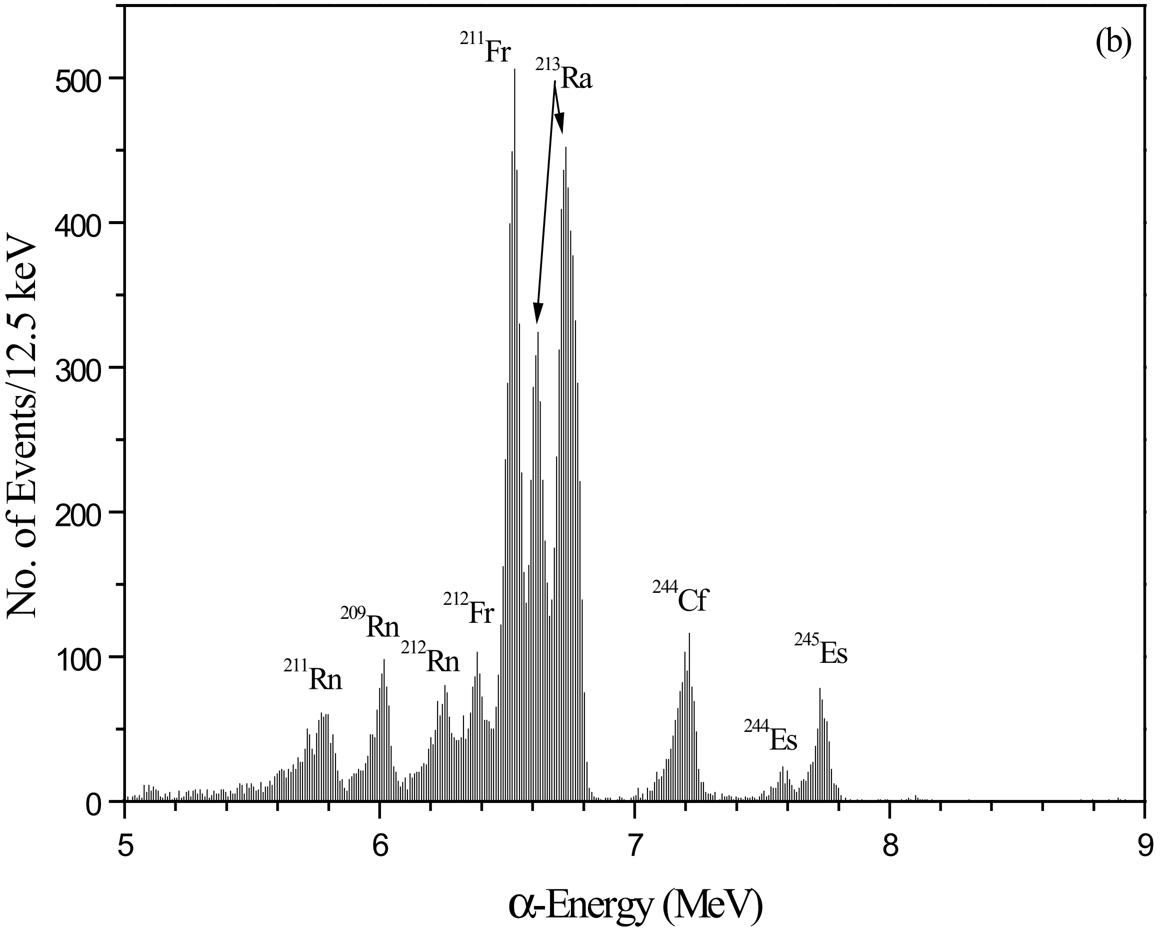
(b)
No. of Events/12.5 keV
α-Energy (MeV)
0
100
200
300
400
500
5
6
7
8
9
211Fr
213Ra
211Rn
209Rn
212Rn
212Fr
244Cf
244Es
245Es

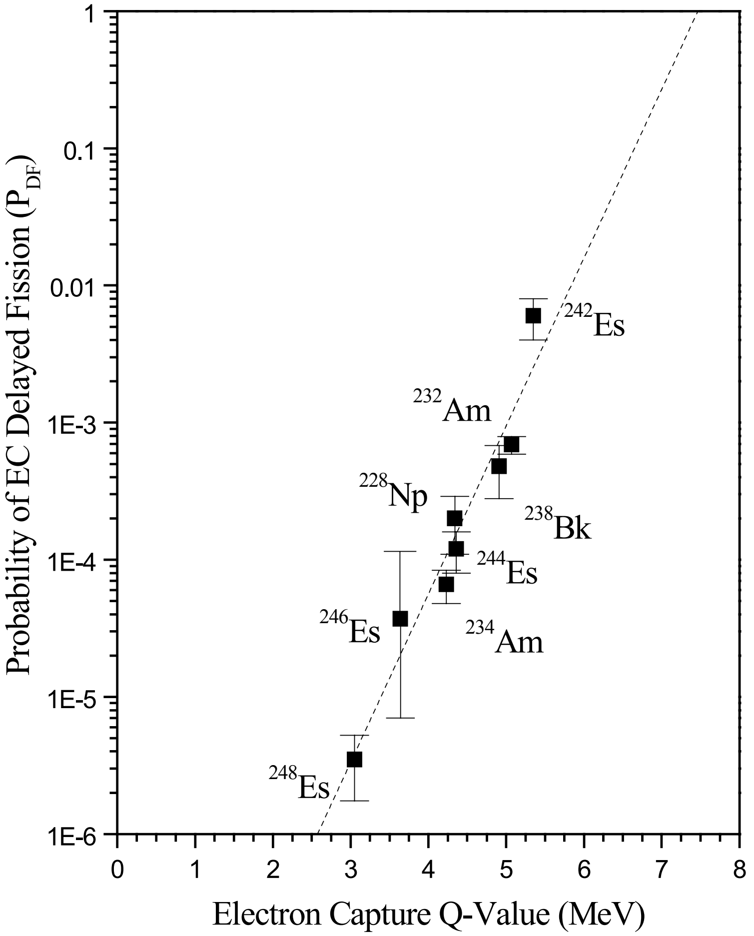

Probability of EC Delayed Fission (P_{DF})
1
0.1
0.01
1E-3
1E-4
1E-5
1E-6
0
1
2
3
4
5
6
7
8
Electron Capture Q-Value (MeV)
^{242}Es
^{232}Am
^{228}Np
^{238}Bk
^{244}Es
^{246}Es
^{234}Am
^{248}Es